

Wire-like Bundle Arrays of Copper Hydroxide Prepared by the Electrochemical Anodization of Cu Foil

Duc-Duong La, Sung Yeol Park, Young-Wook Choi,[†] and Yong Shin Kim*

Department of Applied Chemistry, and Graduate School of Bio-Nano Engineering, Hanyang University, Ansan 426-791, Korea. *E-mail: yongshin@hanyang.ac.kr

[†]Process Materials Research Institute, Cheil Industries Inc., Euiwang 437-711, Korea

Received August 5, 2009, Accepted June 23, 2010

Nanostructured copper compounds were grown by electrochemical anodization of copper foil in aqueous NaOH under varying conditions including electrolyte concentration, reaction temperature, current density, and reaction time. Their morphology and atomic composition were investigated by using SEM, TEM, XRD, EDS and XPS. At the conditions ($[\text{NaOH}] = 1 \text{ M}$, 20°C , 2 mA cm^{-2}), wire-like orthorhombic $\text{Cu}(\text{OH})_2$ nanobundles with an average width of 100 - 300 nm and length of 10 μm were synthesized with the preferential [100] growth direction. Furthermore, when the concentration decreased to 0.5 M NaOH, the 1D nanobundle structure became narrower and longer without any change in compositions or crystalline structure. Side reaction pathways appeared to compete with the 1D nanostructure formation channels: the formation of CuO nanoleaves at 50°C via the sequential dehydration of $\text{Cu}(\text{OH})_2$, CuO/Cu₂O aggregates in 4 M NaOH, and Cu₂O nanoparticles and CuO nanosheets at lower current density.

Key Words: Cu Anodization, Copper hydroxide, Nanobundle, Nanowire

Introduction

One-dimensional (1D) nanostructures (nanowires, nanotubes, nanoribbons) have attracted a great deal of recent attention mainly due to their unique electronic, mechanical, magnetic, and chemical properties.^{1,2} Many methods have been developed for the synthesis of 1D nanomaterials, including template-guided growth, vapor-liquid-solid (VLS) reaction, laser ablation, arc-discharge, and solvothermal treatment.³⁻⁶ However, continuous effort is still necessary to develop new synthetic techniques to control the size and morphology of 1D nanomaterials.

Recently, copper compound films with 1D nanostructures have been prepared with copper foil without the use of a surfactant by a simple liquid-solid reaction. In their pioneering work, Wen *et al.* reported the ability to synthesize $\text{Cu}(\text{OH})_2$ nanoribbons in an aqueous solution of ammonia by coordinating the self-assembly of square planar Cu^{2+} complexes generated from Cu_2S nanowires.⁷ Various copper compound nanostructures, including nanotubes, nanowires, whiskers and nanosheets, have been grown directly by the chemical oxidation of copper foil in alkaline aqueous solutions with an oxidant additive⁸⁻¹¹ or by the electrochemical anodization in an alkaline solutions.¹² In particular, Xu and co-workers successfully prepared $\text{Cu}(\text{OH})_2$ nanowire and nanotube arrays on a copper substrate via the electrochemical route using an electrolyte solution of KOH.¹³ This electrochemical method has an advantage over other methods in that the shape and atomic compositions of final copper compound films can be controlled by means of modulating the potential, reaction time, and the integrated charge passed through the cell. Currently, there is a desire to synthesize size and shape-controlled, and single crystalline 1D $\text{Cu}(\text{OH})_2$.

Rough $\text{Cu}(\text{OH})_2$ nanotube or nanowire films provided an opportunity to form a superhydrophobic surface through sequential surface modification with low surface energy materials

such as *n*-dodecanethiol, perfluorodecyltriethoxysilane and dodecanoic acid.¹⁴⁻¹⁶ This method is a convenient, environmentally friendly, and time-saving process compared to conventional methods. Based on this procedure, copper mesh with superhydrophobic and superoleophilic properties was readily fabricated and applied to a novel filtration device for the separation of water and hydrophobic solvents.^{17,18} In addition, 1D $\text{Cu}(\text{OH})_2$ nanomaterials with a layered structure can be utilized as precursors to form homogeneous, single-crystalline CuO nanoribbons¹⁹ and two-dimensional CuO nanoleaves²⁰ on a large scale via further dehydration processes. These nanoscale CuO materials were widely exploited as a powerful heterogeneous catalysis²¹ and in the fabrication of lithium-copper oxide electrochemical cells.²²

Here we report the electrochemical anodization of copper foil in an aqueous solution of NaOH. Although NaOH is the most common and economic alkaline chemical available, there are no reports describing in detail the use of NaOH as a base for the electrochemical copper anodization. To establish the relationship between the final copper compound film and the experimental conditions used, the anodization protocol was performed sequentially with variations in NaOH concentration, reaction temperature, anodization time, and current density. Optimized conditions for the growth of orthorhombic $\text{Cu}(\text{OH})_2$ nanowires are proposed to be at a 0.5 - 1 M NaOH concentration under a current density of 2 mA cm^{-2} at ambient temperature. Various morphologies and chemical compositions obtained under different experimental conditions were interpreted by the side reaction pathways such as sequential dehydration and Cu_2O formation.

Experimental

The growth of copper compound films was carried out in a

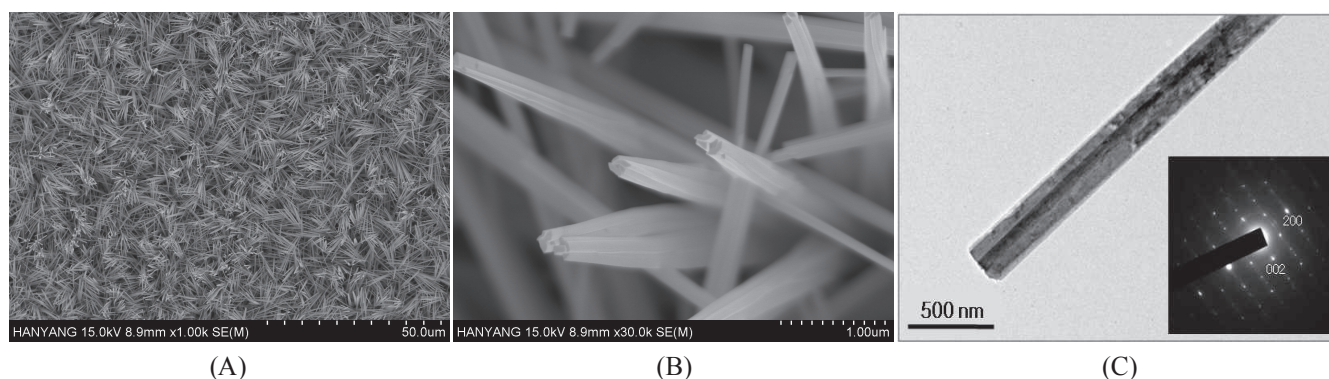


Figure 1. Surface SEM images of copper anodized at a constant current density of 2 mA cm^{-2} in 1.0 M NaOH solution at $20 \text{ }^\circ\text{C}$ with a reaction time of 1300s: (A) low magnification of $\times 1,000$ and (B) high magnification of $\times 30,000$. (C) TEM image corresponding to the individual nanowire bundle of B (insert, SAED).

one-compartment cell connected to the electrochemical analyzer (624C, CH Instruments) under ambient conditions. Copper foil ($2.0 \times 2.0 \text{ cm}^2$) was sequentially washed with acetone, ethanol, 2.0 M HCl , and deionized water for about 5 min each under ultrasonication to remove organic contaminants and an oxide layer on surface. The copper foil was dried using a stream of a compressed air and then immediately used as the working electrode. The counter electrode was a stainless steel sheet with a surface area of approximately 5.0 cm^2 . The electrolyte was an aqueous NaOH solution with concentrations ranging between $0.5 - 4.0 \text{ M}$. The solutions were deaerated by bubbling with dry nitrogen for at least 30 min before experimentations. The copper foil was electrochemically anodized at a constant current density over a $0.1 - 5.0 \text{ mA cm}^{-2}$ range with a typical reaction time of 600 s. A thermostat was used to control cell temperature ranging within $5 - 50 \text{ }^\circ\text{C}$. After anodization, samples were rinsed twice with deionized water and then dried with compressed air before material characterization.

The surface morphology of the as-prepared copper compound films was observed by field emission-scanning electron microscopy (FE-SEM; S-4800, Hitachi) and transmission electron microscopy (JEM-2100F, JEOL). The atomic composition was probed using an equipped X-ray detector through energy dispersive spectroscopy (EDS) and X-ray photoelectron spectroscopy (XPS). X-ray diffraction (XRD) patterns were also obtained using an X-ray diffractometer (D/Max-2500, Rigaku) with $\text{Cu K}\alpha$ radiation ($\lambda = 1.5418 \text{ \AA}$) to confirm crystalline structures.

Results and Discussion

Surface SEM images were observed for the anodized copper foil using of 2 mA cm^{-2} current density in 1 M NaOH at room temperature. The low-magnification image (Fig. 1A) shows vertically-oriented, uniform, and dense distribution of pine-like needles with average length of about $10 \text{ }\mu\text{m}$. However, the tapered tip structures shown in the high-magnification image (Fig. 1B) clearly indicate that the nanoneedle consists of a bundle of several irregular, polygonal wires with an average diameter of $100 - 300 \text{ nm}$. The structure of the anodized copper was further investigated by TEM. Consistent with the SEM

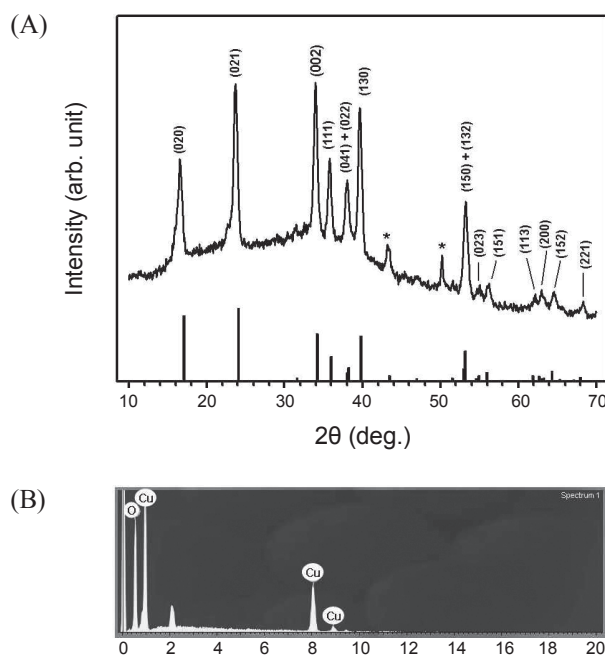


Figure 2. Typical (A) XRD pattern and (B) EDS spectrum of the Cu(OH)_2 nanowire arrays shown in Fig. 1. The lower bar plot in A corresponds to the orthorhombic Cu(OH)_2 phase (JCPDS card No. 80-0656).

observations, the nanoneedle exhibits a layered structure of polygonal wires (see Fig. 1C). The widths of individual nanowires are in the range of $150 - 200 \text{ nm}$.

The anodized copper was further characterized using XRD to confirm its crystal structure and atomic composition. Fig. 2A shows a typical XRD pattern for the sample. All diffraction peaks can be indexed to the orthorhombic Cu(OH)_2 phase with cell parameters of $a = 2.947 \text{ \AA}$, $b = 10.59 \text{ \AA}$ and $c = 5.256 \text{ \AA}$ (JCPDS card No. 80-0656), except those marked with an asterisk, arising from the copper substrate. The selected area electron diffraction (SAED) pattern of a nanobundle (inset of Fig. 1C) demonstrates that single crystalline nanowires, growing along the $[100]$ direction parallel to the longest dimension, were predominantly laid on the (010) plane.

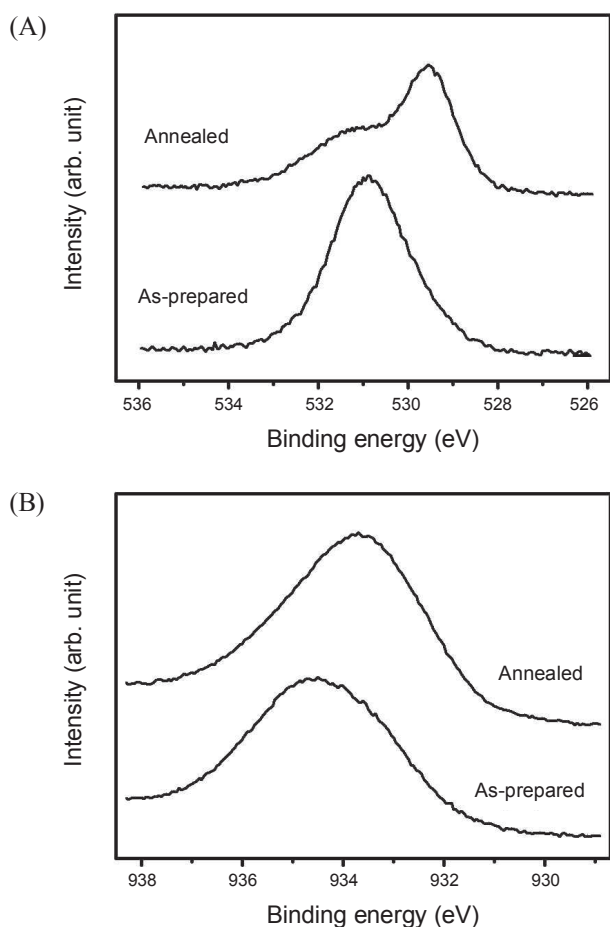
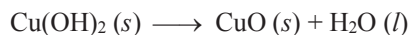


Figure 3. Narrow-scan (A) O 1s and (B) Cu 2p XPS spectra of anodized copper under the optimized conditions. The annealed spectra were obtained after the as-prepared sample underwent 200 °C thermal treatment for 1 hr in air.

The constituent atoms were confirmed to be Cu and O from the EDS spectrum (Fig. 2B). The broad backgrounds are due to Pt being used as a coating layer for SEM observation. The relative Cu : O atomic population ratio was determined to be 1 : 2.1, which is very close to the stoichiometric value of copper hydroxide. XPS measurements were performed to confirm chemical bonding environments of O and Cu atoms in the anodized copper as shown in Fig. 3. The as-prepared sample exhibits the peak positions of 530.9 eV for O 1s and 934.6 eV for Cu 2p, respectively, which can be assigned to a Cu(OH)₂ compound in the light of the values in the literatures.^{23,24} XPS observations also carried out for the sample annealed at 200 °C in air. The thermal treatment results in the chemical shift of Cu 2p peak into low binding energy (933.6 eV), and the additional O 1s peak in low energy (529.5 eV). They can be interpreted with the formation of cupric oxide by the dehydration process of as-formed Cu(OH)₂ as previously reported.¹⁹



Moreover, it was observed that Cu(OH)₂ nanostructures were transformed into corresponding CuO without any noticeable change in morphology during the post-thermal treatment. Con-

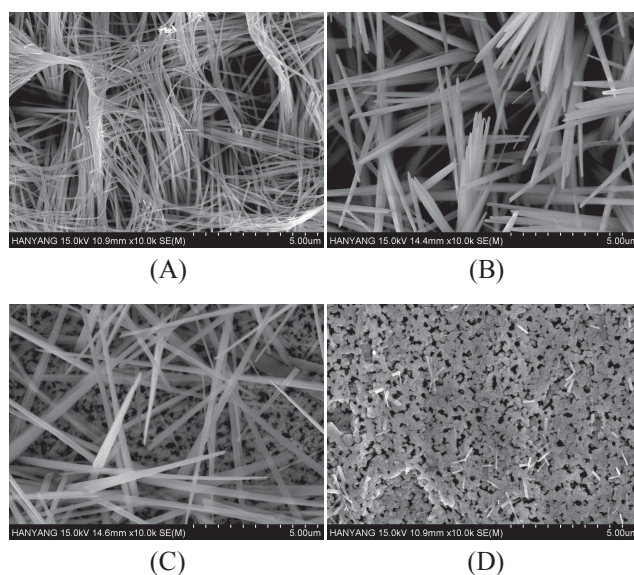
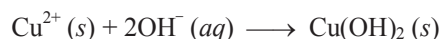


Figure 4. SEM images of copper foil anodized in different NaOH concentrations: (A) 0.5 M, (B) 1.0 M, (C) 2.0 M and (D) 4.0 M. All were generated under the same current density of 2 mA cm⁻² and reaction time of 600 s at 20 °C.

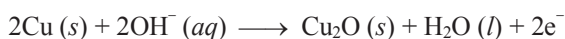
sequently, the bundle arrays of orthorhombic Cu(OH)₂ polygonal nanowires were mainly formed from the electrochemical Cu anodization under the conditions of current density of 2 mA cm⁻² in 1 M NaOH at room temperature.

The plausible mechanism for the formation of nanowire-bundle structures can be given on the ground of previous results obtained in the alkaline oxidant solution system.^{7,8} When an electrical potential was applied to copper foil in NaOH solution, its surface underwent an electrochemical oxidation process:



This reaction was accompanied by the evolution of gas bubbles from the counter electrode surface, supporting the occurrence of a reduction reaction such as $2\text{H}^+ + 2e^- \rightarrow \text{H}_2 (g)$. The nucleation of Cu(OH)₂ began from localized regions of supersaturation where crystalline Cu(OH)₂ started to grow and was assembled into the observed bundle structure. Generally, the morphology of a crystal is determined by the different growth speeds of crystal faces under a nonequilibrium oxidation system. The orthorhombic Cu(OH)₂ structure was known to consist of chains in the (001) planes, characterized by the square-planar coordination of Cu²⁺ ions with strong σ bonds. The Cu²⁺ ions then formed two longer bonds with two OH⁻ groups from neighboring chains along the *c* axis, forming a corrugated sheet parallel to (010). The two-dimensional sheets were stacked through the relatively weak hydrogen bond interactions, and therefore became a three-dimensional crystal. The growth speed of such a crystal is normally proportional to $1/d_{hkl}$.²⁵ The interplanar distance of 10.59 Å for the (010) planes was the longest whereas the (100) distance of 2.947 Å was the shortest. Therefore, Cu(OH)₂ nanowires were believed to grow along the [100] direction with the arrangement parallel to the (010) planes.

The concentration of nucleophile OH^- ions may have a substantial effect on the growth mechanism, ultimately determining the morphology of the resultant copper compound film. We examined the influence of NaOH concentration on the morphology of final copper film products. SEM images show the morphology change of copper compound films formed with varying the NaOH concentration over the 0.5 - 4 M range (Fig. 4). These samples were anodized under the same conditions (current density of 2 mA cm^{-2} , temperature of 20°C , and a reaction time of 600 s) except for the NaOH concentration. These results clearly exhibit that the morphology of anodized Cu was strongly dependent on NaOH concentration. The 1 M SEM image (Fig. 4B) shows the nanoneedle shape identical to those of the sample prepared with the same concentration and a longer reaction time of 1300 s (Fig. 1). The long reaction time simply results in an increase in length without a noticeable change in width. In low 0.5 M concentration, the surface structure still maintained a wire-like shape with an average width of 100 nm as shown in Fig. 4A. Moreover, a relative Cu : O atomic ratio of 1 : 2.3 determined by EDS supported the formation of copper hydroxide. However, there were some distinct differences in shape: 1D nanostructures, consisting of a bundle of a few nanoribbons in high-magnification images, were narrower and longer than those produced at 1M NaOH. These observations suggest that the decrease in NaOH concentration resulted in the formation of a more elongated sheet along the [100] direction and the resultant structures were nanoribbons rather than nanowires. As the NaOH concentration increased from 1 M to 4 M, nanowire structures gradually disappeared from the surface (see Figs. 4B - 4D). At 4 M NaOH, the copper surface was predominantly covered with aggregated particles. The relative Cu : O atomic ratio determined by EDS was 1 : 1.1 and 1 : 0.2 for 2 M and 4 M NaOH, respectively. Furthermore, XRD peaks of cubic Cu_2O and monoclinic CuO were observed in the sample anodized in 4 M NaOH. This implies that the nanoparticle agglomerates formed under high NaOH concentration were no longer orthorhombic $\text{Cu}(\text{OH})_2$ with 1D nanostructure. The sequential dehydration of $\text{Cu}(\text{OH})_2$, as observed above in the thermal treatment process of as-prepared $\text{Cu}(\text{OH})_2$, must be responsible for the CuO formation. The electrochemical Cu_2O formation on Cu foil was previously reported,^{13,26} and could be understood by the following reaction:



Therefore, under strong basic conditions, the Cu^{2+} ions generated by electrochemical anodization favored the formation of cuprous and cupric oxide instead of copper hydroxide.

The NaOH concentration-dependent change in electrochemical copper anodization can be summarized as follows: (1) the favorable formation of a $\text{Cu}(\text{OH})_2$ sheet occurs in NaOH concentrations less than 1 M *via* the anodization followed by the OH^- addition reaction, (2) the sheets formed in 1 M NaOH have wire-like nanostructures whereas the 0.5 M anodization leads to the production of more anisotropic sheets (ribbon-like nanostructures), and (3) Cu_2O and CuO particles are favorably formed but become aggregated lumps with cavities near the surface under the electrolyte concentrations higher than 4 M.

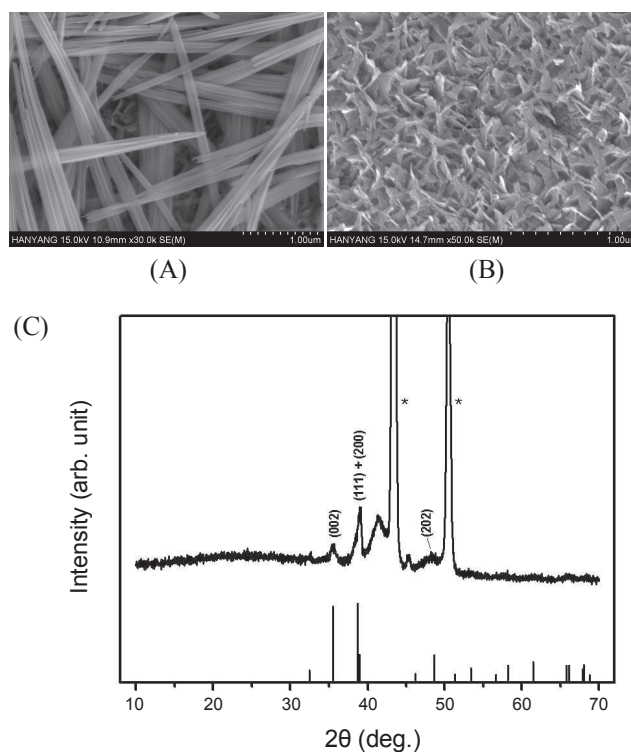


Figure 5. SEM images of samples obtained by anodizing a copper foil at different temperatures using 0.5M NaOH, current density of 2 mA cm^{-2} , and a reaction time of 600s: (A) 35°C and (B) 50°C . And (C) XRD pattern of the 50°C sample. The lower bar plot corresponds to the monoclinic CuO phase (JCPDS card No. 80-1916).

The anodization mechanism of Cu foil was further investigated by analyzing the effect of reaction temperature variation in the range of $5 - 50^\circ\text{C}$. The electrochemical anodization carried out in 0.5 M NaOH, which has an advantage to prepare a superhydrophobic surface due to the high aspect ratio in nanobundle structures. The surface morphology of a sample anodized at 5°C was observed to be similar to that of 20°C , showing 1D $\text{Cu}(\text{OH})_2$ nanobundle arrays. The only difference between the samples was in length: the average length at 5°C was approximately half that of what was observed at 20°C , indicating that the growth mechanism is nearly identical at these temperatures, but the growth rate becomes slower as temperature decreases below 20°C . In contrast, there was considerable change in shape when the reaction temperature increased above 20°C . Figs. 5A and 5B show SEM image of the samples anodized at 35°C and 50°C , respectively. Unusual leaf-like nanostructures were observed in the 50°C image, while both nanobundles and nano-sized leaves displayed near the surface. It suggests that an additional reaction pathway exists as the temperature increases from 20°C to 50°C . The atomic composition and crystalline structure of the leaf-like nanostructures were determined using EDS and XRD analyses, respectively. The leaf-like arrays were comprised of Cu and O atoms with a Cu : O atomic ratio of 1 : 1.2, close to the stoichiometry of cupric oxide. The XRD pattern shown in Fig. 5C clearly supports the existence of a monoclinic CuO phase (JCPDS card No. 80-1916). The CuO formation maybe comes from the sequential dehydration process, $\text{Cu}(\text{OH})_2 (s) \rightarrow \text{CuO} (s) + \text{H}_2\text{O} (l)$.

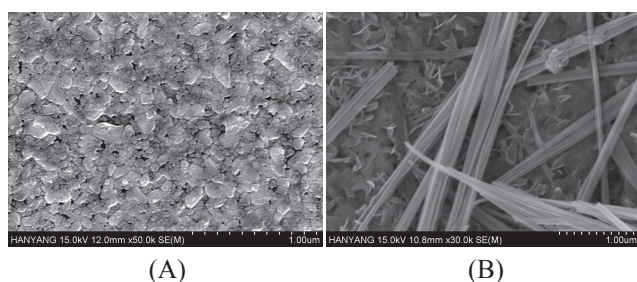


Figure 6. SEM images of copper foil anodized at low current densities, (A) 0.1 mA cm^{-2} and (B) 0.5 mA cm^{-2} , using 0.5 M NaOH , reaction temperature of $20 \text{ }^\circ\text{C}$, and a reaction time of 600 s .

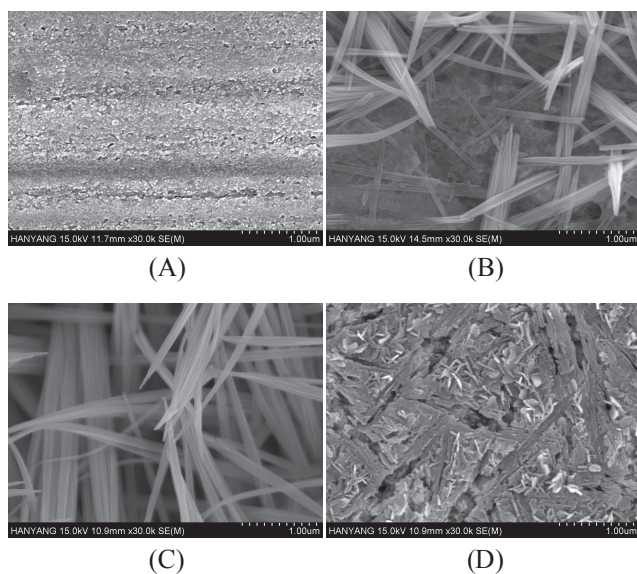


Figure 7. SEM images of samples obtained by anodizing a copper foil with different reaction times at room temperature using 0.5 M NaOH , and current density of 2 mA cm^{-2} : (A) 30 s , (B) 60 s , (C) 300 s , and (D) 1800 s .

As a result, the samples anodized at different reaction temperatures were characterized by differing chemical compositions and nanostructures. Therefore, careful temperature regulation, in addition to the control of NaOH concentration, is required to obtain a well-defined copper compound film in composition and structure. With increasing reaction temperature, the growth rate for the wire-like $\text{Cu}(\text{OH})_2$ formation gradually increased while the sequential dehydration rate became favorable at above $50 \text{ }^\circ\text{C}$.

The influences of current density, ranging from $0.1 - 10 \text{ mA cm}^{-2}$, on the anodization mechanism was also investigated. Fig. 6A and B show two SEM images for the anodized surface at the low current densities of 0.1 and 0.5 mA cm^{-2} , respectively. Black irregular nanoparticles appeared at 0.1 mA cm^{-2} , while the 0.5 mA cm^{-2} sample exhibited a blue surface with sparse 1D nanowires on randomly arranged sheet arrays. This mixed appearance was still observed at 1 mA cm^{-2} , and was then no longer seen at 2 mA cm^{-2} due to complete surface coverage by the surface nanowires. With the aid of EDS and XRD analyses, it was confirmed that the black nanoparticles were crystalline cuprous oxides, and that the nanosheets might be cupric

or cuprous oxides. Electrochemical anodization processes were known to form a porous Cu_2O layer at first, and then $\text{Cu}(\text{OH})_2$ or CuO films on it.^{27,28} Bouillon *et al.* found that only CuO was observed at low current density ($< 0.5 \text{ mA cm}^{-2}$), and $\text{Cu}(\text{OH})_2$ was dominant at above 0.8 mA cm^{-2} .²⁹ In the light of these previous reports, we can interpret our results as followings: 1) at 0.1 mA cm^{-2} , Cu foil is covered with only the porous Cu_2O particles because of a small current density for the growth of $\text{Cu}(\text{OH})_2$ or CuO films; 2) sheet-shape CuO mainly grows at 0.5 mA cm^{-2} ; 3) the growth of 1D $\text{Cu}(\text{OH})_2$ nanostructures, competing with the formation of CuO , become more favorable with increasing a higher current density between $1 - 2 \text{ mA cm}^{-2}$. Gas bubbles were evolved from the surface of the copper foil in the electrochemical anodization above 5 mA cm^{-2} . This phenomenon can be interpreted by the electrolysis process:



Thus, the optimized current density for the formation of a compact blue 1D $\text{Cu}(\text{OH})_2$ film is approximately 2 mA cm^{-2} .

Fig. 7 shows SEM images as a function of anodization time in order to observe the change in surface morphology. The electrochemical anodization was performed using the following conditions; 0.5 M NaOH , current density of 2 mA cm^{-2} , and temperature of $20 \text{ }^\circ\text{C}$. There was no discernable change until a reaction time of 30 s was reached. As the reaction time was increased, nanobundles started to appear and gradually become longer and denser between 60 and 600 s . The nanobundles were observed to be completely removed from the surface after 1800 s . The initial incubation time longer than 30 s is required to start the growth of 1D $\text{Cu}(\text{OH})_2$. The delayed growth can be understood with the initial growth of a Cu_2O base layer mentioned above. At long reaction time such as 1800 s , long nanobundles seem to undergo side reactions such as agglomeration among the formed nanobundles and dissolution into the electrolyte solution, probably due to a lowered nanowire growth rate.

Conclusion

We have synthesized orthorhombic copper hydroxide arrays with 1D nanostructures by anodizing copper foil in an aqueous NaOH solution. Optimized conditions for the wire-like nanobundle formation were found to be $0.5 - 1 \text{ M NaOH}$ at a reaction temperature of $20 \text{ }^\circ\text{C}$ and current density of 2 mA cm^{-2} . The growth was interpreted by the formation of anisotropic $\text{Cu}(\text{OH})_2$ lamellates parallel to the (010) planes with the growth direction of [100]. In addition, other copper compound nanostructures of Cu_2O agglomerates and CuO nano-leaves were formed under non-optimized conditions. These observations suggest that there are side reactions that hamper the nanobundles formation. These include the sequential dehydration of as-formed $\text{Cu}(\text{OH})_2$ to form cupric oxide at high temperature, the Cu_2O formation at low current density, and the Cu_2O and CuO formations at high NaOH concentration. Consequently, single crystalline quasi-aligned $\text{Cu}(\text{OH})_2$ nanowires can be prepared on a large scale by using this simple electrochemical anodization process, where the length and shape of the 1D nanostructures are easily controllable based upon reaction conditions.

This protocol for the production of 1D Cu(OH)₂ nanobundle arrays can be widely utilized to prepare promising CuO nanomaterials and superhydrophobic surfaces.

Acknowledgments. This research was mainly supported by the National Research Foundation of Korea (NRF) funded by the Ministry of Education, Science and Technology (No. 2009-0090894 and No. 2009-0083917). YSK thanks the financial support of the Ansan-si project program.

References

1. Cao, G. *Nanostructures & nanomaterials: Synthesis, Properties & Application*; Imperial college press: London, 2004; pp 110-173.
2. Ozin, G. A.; Arsenault, A. C. *Nanochemistry: A Chemical Approach to Nanomaterials*; RSC publishing: Cambridge, 2005; pp 167-265.
3. Ajayan, P. M.; Stephan, O.; Redlich, Ph.; Colliex, C. *Nature* **1995**, *375*, 564.
4. Ha, W.; Fan, S.; Li, Q.; Hu, Y. *Science* **1997**, *277*, 1287.
5. Xia, Y.; Rogers, J. A.; Paul, K. E.; Whitesides, G. M. *Chem. Rev.* **1999**, *99*, 1823.
6. Xia, Y.; Yang, P.; Sun, Y.; Wu, Y.; Brian, M.; Byron, G.; Yin, Y.; Kim, Y.; Yan, H. *Adv. Mater.* **2003**, *15*, 353.
7. Wen, X.; Zhang, W.; Yang, S. *Nano Lett.* **2002**, *2*, 1397.
8. Zhang, W.; Wen, X.; Yang, S.; Berta, Y.; Wang, Z. L. *Adv. Mater.* **2003**, *15*, 822.
9. Zhang, W.; Wen, X.; Yang, S. *Inorg. Chem.* **2003**, *42*, 5005.
10. Wen, X.; Zhang, W.; Yang, S. *Langmuir* **2003**, *19*, 5898.
11. Wen, X.; Xie, Y.; Choi, C. L.; Wan, K. C.; Li, X.-Y.; Yang, S. *Langmuir* **2005**, *21*, 4729.
12. Shoesmith, D. W.; Rummery, T. E.; Owen, D.; Lee, W. *J. Electrochem. Soc.* **1976**, *123*, 790.
13. Wu, X.; Bai, H.; Zhang, J.; Chen, F.; Shi, G. *J. Phys. Chem. B* **2005**, *109*, 22836.
14. Pan, Q.; Jin, H.; Wang, H. *Nanotechnology* **2007**, *18*, 355605.
15. Wu, X.; Shi, G. *J. Phys. Chem. B* **2006**, *110*, 11247.
16. Chen, X.; Kong, L.; Dong, D.; Yang, G.; Yu, L.; Chen, J.; Zhang, P. *Appl. Surf. Sci.* **2009**, *255*, 4015.
17. Pan, Q.; Wang, M.; Wang, H. *Appl. Surf. Sci.* **2008**, *254*, 6002.
18. Wang, S.; Song, Y.; Jiang, L. *Nanotechnology* **2007**, *18*, 015103.
19. Hou, H.; Xie, Y.; Li, Q. *Cryst. Growth Des.* **2005**, *5*, 201.
20. Xu, H.; Wang, W.; Zhu, W.; Zhou, L.; Ruan, M. *Cryst. Growth Des.* **2007**, *7*, 2720.
21. Reitz, J. B.; Solomon, E. I. *J. Am. Chem. Soc.* **1998**, *120*, 11467.
22. Wang, H.; Pan, Q.; Zhao, J.; Yin, G.; Zuo, P. *J. Power Sources* **2007**, *167*, 206.
23. Hoque, E.; DeRose, J. A.; Houriet, R.; Hoffmann, P.; Mathieu, H. *J. Chem. Mater.* **2007**, *19*, 798.
24. <http://www.lasurface.com>.
25. Vere, A. W. In *Crystal Growth: Principles and Progress*; Dobson, P. J., Ed.; Plenum Press: New York, 1987; p 17.
26. Singh, D. P.; Neti, N. R.; Sinha, A. S. K.; Srivastava, O. N. *J. Phys. Chem. C* **2007**, *111*, 1638.
27. Becerra, J. G.; Salvarezza, R. C.; Arvia, A. J. *Electrochimica Acta* **1988**, *33*, 613.
28. Shoesmith, D. W.; Rummery, T. E.; Owen, D.; Lee, W. *J. Electrochem. Soc.* **1976**, *123*, 790.
29. Bouillon, F.; Piron, J.; Stevens, J. *Bull. Soc. Chim. Belges* **1958**, *67*, 643.